

RESEARCH PAPER



Human placental hematopoietic stem cell derived natural killer cells (CYNK-001) mediate protection against influenza a viral infection

Joseph Gleason, Yuechao Zhao, Irene Raitman, Lin Kang, Shuyang He, and Robert Hariri

Celularity Inc., Florham Park, New Jersey, NJ, USA

ABSTRACT

Influenza A virus (IAV) infections are associated with a high healthcare burden around the world and there is an urgent need to develop more effective therapies. Natural killer (NK) cells have been shown to play a pivotal role in reducing IAV-induced pulmonary infections in preclinical models; however, little is known about the therapeutic potential of adoptively transferred NK cells for IAV infections. Here, we investigated the effects of CYNK-001, human placental hematopoietic stem cell derived NK cells that exhibited strong cytolytic activity against a range of malignant cells and expressed high levels of activating receptors, against IAV infections. In a severe IAV-induced acute lung injury model, mice treated with CYNK-001 showed a milder body weight loss and clinical symptoms, which led to a delayed onset of mortality, thus demonstrating their antiviral protection *in vivo*. Analysis of bronchoalveolar lavage fluid (BALF) revealed that CYNK-001 reduced proinflammatory cytokines and chemokines highlighting CYNK-001's anti-inflammatory actions in viral induced-lung injury. Furthermore, CYNK-001-treated mice had altered immune responses to IAV with reduced number of neutrophils in BALF yet increased number of CD8+ T cells in the BALF and lung compared to vehicle-treated mice. Our results demonstrate that CYNK-001 displays protective functions against IAV via its anti-inflammatory and immunomodulating activities, which leads to alleviation of disease burden and progression in a severe IAV-infected mice model. The potential of adoptive NK therapy for IAV infections warrants clinical investigation.

ARTICLE HISTORY

Received 27 December 2021
Revised 4 March 2022
Accepted 17 March 2022

KEYWORDS

Virus; influenza a;
inflammation; natural killer
cells

Introduction

Influenza A virus (IAV) infections are associated with a high healthcare burden around the world.¹ Globally, its epidemics typically occur during the cold season in temperate regions when low humidity and temperature ambient conditions are suggested to prolong virus shedding and transmission, while in subtropical and tropical regions the less clearly defined influenza seasons allow recurrent infections through the year. Overall, seasonal IAV affects up to 10% of the adult population and 20% of children annually and displays a substantial morbidity.² Vaccination remains the most effective means to prevent and control IAV infections; however, annual vaccinations are limited in efficacy due to rapid antigenic evolution in the hemagglutinin (HA) glycoprotein. Influenza vaccine effectiveness in the 2018–2019 influenza season in the United States was 47% overall and 46% against IAV (H1N1),³ respectively. Alternative therapies to control emerging IAV are urgently needed.

Natural Killer (NK) cells are innate immune cells with an important role in early host response against various pathogens. Multiple NK cell receptors are involved in the recognition of infected cells, including NKG2D, DNAM-1 and the natural cytotoxicity receptors (NCRs) NKp30, NKp44 and NKp46, which bind common stress ligands or pathogen-associated molecules.⁴ Using these immune receptors, NK cells are able to recognize and spontaneously kill 'stressed' cells, such as virally infected or tumor cells, without prior sensitization. In addition, superiorities of NK cell-based therapies over T cells include better safety such as absence or minimal cytokine release syndrome (CRS) and graft-versus-host

disease (GVHD), engaging various mechanisms for stimulating cytotoxic function, and high feasibility for 'off-the-shelf' manufacturing.⁵ Abnormal cells trigger NK cell activation either through the loss of self-identifying molecules, such as major histocompatibility complex (MHC) class I, that bind to inhibitory receptors on the NK cells or by upregulating the expression of ligands for activating receptors on NK cells that can overcome the inhibitory signals. Various viral glycoproteins expressed by enveloped viruses are specifically recognized by NCRs.^{6,7} Activated NK cells release cytokines with potent antiviral activity, such as interferon gamma (IFN γ) and tumor necrosis factor alpha (TNF α), as well as cytotoxic granules containing perforin and granzyme B.⁸

Recent studies have demonstrated that there is robust activation of NK cells during viral infection, and that the depletion of NK cells aggravates viral pathogenesis.^{9–13} Many mouse models of influenza infection also implicate a protective role for NK cells during infection.^{11–15} However, in high dose severe infection models, murine NK cells appeared to play a detrimental role, contributing to influenza pathogenesis.^{16,17} In humans, it has been reported that the number of NK cells decreased upon seasonal IAV infection in peripheral blood¹⁸ and NK cell lymphopenia in the peripheral blood and lung was associated with disease severity of 2009 pandemic H1N1 infection.^{19,20} These findings not only suggest that further studies are required to fully understand important roles of NK cells against IAV infection, but also highlight adoptive NK cell therapy may provide clinical benefits against IAV infection.

Since little is known about the therapeutic potential of adoptively transferred human NK cells against IAV infections, here we investigated antiviral function of adoptively transferred CYNK-001, a culture-expanded NK cell population derived from human placental hematopoietic stem cells, and its effects on host immune responses to IAV infection. CYNK-001 is currently being studied in four ongoing clinical trials: Phase I study in patients who have relapsed and/or refractory AML (NCT04310592), Phase I/II study for multiple myeloma (MM) (NCT04309084), Phase I study for glioblastoma multiforme (GBM) (NCT04489420) and Phase I/II study for coronavirus disease 2019 (COVID-19) (NCT04365101). In this study by using an immunocompetent mouse model with severe IAV-infection, we found that adoptive transfer of CYNK-001 displays protective functions against IAV, by suppression of inflammation and immunomodulation in disease-injured lungs without causing host immunotoxicity.

Materials and methods

CYNK-001 cell culture

CYNK-001 was derived by expanding and differentiating placental hematopoietic stem/progenitor CD34+ cells in a 35-day culture process. Placental CD34+ cells were cultivated in the presence of various human cytokines for 35 days to generate CYNK-001 under current good manufacturing practices standards, followed by release testing. Cytokine cocktail containing IL-2, IL-15, SCF and IL-7 were used for placental CD34+ cells expansion and differentiation as described before.²¹ Cells were harvested following the 35-day expansion and differentiation process and then frozen as a drug substance.

In vitro characterization of CYNK-001

CYNK-001 cells with NK cell purity of $\geq 90\%$ CD56+CD3-, were used in this assay. Frozen CYNK-001 cells were thawed and washed in staining buffer, phosphate buffered saline (PBS) (10,010–023, Gibco) containing 10% FBS (10,082–147, Gibco). 1×10^6 CYNK-001 cells were stained with LIVE/DEAD® Fixable Aqua Dead Cell Stain (L34966, Invitrogen) in PBS and then blocked with a solution containing Purified Mouse IgG2a, κ Isotype Control (555,571, BD), Human BD Fc Block™ (564,219, BD) and BD Horizon™ Brilliant Stain Buffer (563,794, BD). Fluorophore-conjugated antibodies from BD, Miltenyi Biotec and Biolegend were diluted in staining buffer according to manufacturers' instructions. The following antibodies were used: CD226 (Clone: D \times 11 559,789, BD), CD337 (Clone: p30–15 563,385, BD), CD335 (Clone: 9-E2 563,230, BD), CD56 (Clone: 5.1H11 362,510, BioLegend), CD3 (Clone: SK7 560,176, BD), CD14 (Clone: M ϕ P9, 641,394, BD), CD19 (Clone: SJ25C1 641,395, BD), CD336 (Clone: p44–8 744,300, BD), CD314 (Clone: BAT221 130-092-673, Miltenyi Biotec). Samples were acquired on Cytex® Aurora flow cytometer (Cytex, CA, US) and data analyzed on FlowJo™ Software (BD, Version 10.7.2). Two independent experiments had been performed from the six CYNK-001 donors.

Influenza a virus

Influenza virus A/Puerto Rico/8/34 (IAV PR8) H1N1 virus were obtained from ATCC (VR-95). They were grown in Madin–Darby canine kidney (MDCK) cells and then aliquoted and stored at -80°C . Viruses were titrated in MDCK cells [50% tissue culture infective dose (TCID₅₀)] as described elsewhere.²²

Murine influenza model

Animal study was conducted by contract research organization, Pharmaseed Ltd, and study was approved by the institutional IACUC and safety committees. Female Balb/c mice, 6–8 weeks old, were obtained from Envigo RMS (Israel) Ltd and maintained under pathogen-free conditions with a 12-hour light cycle. On day 0, mice were anesthetized using Ketamine/Xylazine injection (90/10 mg/kg, SC). A total volume of 50 μL of IAV PR8 suspension containing 2500 PFU was administered intranasally. Weight was recorded daily, and mice were euthanized either on day 7 or when euthanasia criterion was met with more than 20% weight loss from day 0. The animals were observed for clinical symptoms daily with special attention to piloerection, hunched posture and hindlimb paralysis. Scoring of the disease progression was performed according to Table 1.

CYNK-001 preparation and administration

On day 1 and day 3, cryopreserved CYNK-001 cells were thawed in a 37°C water bath. After centrifugation, CYNK-001 cells were resuspended in PBS. Cell viability was determined by trypan blue, with an average of viability of approximately 95%. PBS or 1×10^7 CYNK-001 cells were intravenously administered into the tail vein at a dose volume of 200 μL on day 1 and day 3. A total of 26 mice were randomly assigned to PBS control ($n = 13$) and CYNK-001 ($n = 13$) groups. Five mice from each group were euthanized on Day 3, 4 hours post the second dose of PBS or CYNK-001.

Measurement of cytokines in bronchoalveolar lavage fluid (BALF)

BALF was collected from PBS and CYNK-001-treated mice. Lungs were flushed multiple time with a total volume of 1.3 ml ice-cold sterile Hanks' Balanced Salt Solution (HBSS) with 3 mM EDTA, pH 7.2. The obtained fluid was centrifuged at 800 g for 10 min at 4°C . The cells were cryopreserved in CryoStor 10 cryopreservation media (Sigma, C2874) and the supernatant was stored in -80°C . Mouse cytokines in BALF were measured using a Milliplex MAP Cytokine/Chemokine Magnetic Bead

Table 1. Clinical symptom score.

Clinical Sign*	Points
Hunched posture	3
Ruffled fur (piloerection)	3
Greater than 20% body weight loss	10
Neurological symptoms (hind-limb paralysis)	10

Note: *Moribund animals or animals obviously in pain, showing signs of severe and enduring distress, hind-limb paralysis and animals showing a decrease of body weight larger than 20% from initial body weight determination or 10% decrease between successive weighing were euthanized.

Panel from Millipore Sigma (MYCTOMAG-70K) and analyzed using Belysa curve fitting software. The presence of human cytokines was evaluated using a Milliplex MAP Human CD8+ T Cell Magnetic Bead Panel from Millipore Sigma (HCD8MAG-15K).

Immune cell phenotyping in BALF

Cryopreserved BAL cells were thawed, washed with PBS, and stained with Aqua Live/Dead viability dye according to the manufacturer's instructions. Cells were blocked in FACS Buffer (PBS with .5% BSA and 2 mM EDTA) using mouse Fc Block (clone 2.4 G) from BD Biosciences and then stained for 30 min at 4°C with the following antibodies: anti-CD45-BV605 (clone 30-F11), anti-Ly6 G-AF700 (clone 1A8), anti-CD11b-BV421 (clone M1/70), anti-CD11c-BV786 (clone HL3), anti-CD3-BUV496 (clone 145-2C11), anti-CD4-PerCP (clone RM4-5), anti-CD8-APC-H7 (clone 53-6.7), anti-MerTK-APC (clone 2B10C42), anti-CD64-PE-Cy7 (clone X54-5/7.1), anti-F4/80-PE (clone T45-2342), anti-IA/IE-FITC (clone M5/114.15.2), and anti-Siglec-F-PE-CF594 (clone E50-2440). Cell profiles were acquired on a BD LSR Fortessa X20 with beads used for compensation of spectral overlap. Fluorescence Minus One (FMO) for markers were used as gating controls. Immune cell populations were identified based on previously described cell surface markers²³ with slight modifications (Table 2). Data were analyzed using FlowJo (V10, TreeStar).

Immunohistochemistry

Formaldehyde fixed, paraffin embedded lung samples were sectioned to 4-micron thickness and placed on slides for immunohistochemical evaluation. Sectioned lung tissues were stained for the following murine cell markers: CD3, CD4, CD8, and CD68. Alkaline phosphatase (AP)- and 3,3'-Diaminobenzidine (DAB)-based methods were used for single and/or dual staining. Quantitative analysis of the number of positive cells in separate fields was reported.

Statistical analysis

GraphPad Prism 9.3.1 (GraphPad Prism Software, Inc.) was used to calculate statistics one-way ANOVA, paired and unpaired *t* test methods. Data were expressed as the mean ± SEM. Statistical significance was shown as *, *P* < .05; **, *P* < .01 and ***, *P* < .001.

Results

In vitro characterization of CYNK-001 cells

CYNK-001 is a culture-expanded NK cell population derived from human placental hematopoietic stem cells with the nominal NK surface phenotype of CD3⁻ CD14⁻ CD19⁻ CD56⁺ (Figure 1a). The activating receptors of NK cells such as NKp46, NKp44, and NKp30, have been implicated in functionally arming NK cells following influenza virus infection via binding with influenza virus hemagglutinin (HA),⁷ and our CYNK-001 exhibited strong cytolytic activity against a wide range of tumor cell lines.²⁴ Therefore, we further validated high expression levels of activating receptors including NKp30, NKp44, NKp46, DNAM-1 and NKG2D as a basal phenotype for CYNK-001 NK cells (Figure 1b and 1c). Taken together, these data suggest that CYNK-001 cells may recognize virally infected cells through the binding of IAV HA with NK cell receptors such as NKp44, and exert cytotoxic elimination of the source of infection. Further studies are required to explore this hypothesis.

CYNK-001 confers *in vivo* resistance to severe IAV infection

To evaluate *in vivo* effects of CYNK-001 on acute and severe lung injury and inflammation, we chose a high-dose IAV-infection mouse model, in which CYNK-001 (1 × 10⁷ cells/mouse) was intravenously infused at 1- and 3-days post infection (dpi) as described in Figure 2a.

As early as 3 dpi, infection caused rapid weight loss (Figure 2b) with increased clinical symptoms characterized by hunching and ruffled fur (Figure 2c and Table 1). Notably, mice received CYNK-001 cells had reduced weight loss and milder clinical symptoms compared to PBS-treated mice. Consistent with these findings, mice treated with CYNK-001 showed a delayed onset of mortality: At 4 dpi, all mice in the CYNK-001-treated group were alive whereas 37.5% mortality rate occurred to the PBS-treated group (Figure 2d), although the difference was not statistically significant (*p* = .0547, χ^2 test). These results indicate CYNK-001-mediated resistance to the disease progression caused by severe IAV infection in mice.

The presence of CYNK-001 in Balb/c lungs was only detectable at 4 hours post i.v. infusion by digital PCR with an hTERT primer/probe specific for human gDNA (Fig. S2), while human cytokines secreted by CYNK-001 cells were undetectable in the BALF and plasma samples at 3 and 6 dpi (data not shown).

Table 2. Immunophenotypes of BALF cells.

Cell population	Immunophenotype
Neutrophils	CD45 ⁺ , Ly6 G ⁺
CD8 ⁺ T cells	CD45 ⁺ , Ly6 G ⁻ , Myeloid ⁻ (CD11b ⁻ and CD11c ⁻), CD3 ⁺ , CD8 ⁺
CD4 ⁺ T cells	CD45 ⁺ , Ly6 G ⁻ , Myeloid ⁻ (CD11b ⁻ , and CD11c ⁻), CD3 ⁺ , CD4 ⁺
NK Cells	CD45 ⁺ , Ly6 G ⁻ , Myeloid ⁺ (CD11b ⁺ and/or CD11c ⁺), SSC ^{lo} , IA/IE ⁻ , CD64 ⁻ , CD11b ^{int}
Total Macrophages	CD45 ⁺ , Ly6 G ⁻ , Myeloid ⁺ (CD11b ⁺ and/or CD11c ⁺), SSC ^{hi} , IA/IE ⁺ , MerTK ⁺ , CD64 ⁺
Alveolar Macrophages	CD45 ⁺ , Ly6 G ⁻ , Myeloid ⁺ (CD11b ⁺ and/or CD11c ⁺), SSC ^{hi} , IA/IE ⁺ , MerTK ⁺ , CD64 ⁺ , CD11b ^{lo/neg} , CD11c ^{hi} , F4/80 ⁺ , Siglec-F ⁺
Interstitial Macrophages	CD45 ⁺ , Ly6 G ⁻ , Myeloid ⁺ (CD11b ⁺ and/or CD11c ⁺), SSC ^{hi} , IA/IE ⁺ , MerTK ⁺ , CD64 ⁺ , CD11b ^{hi} , CD11c ^{lo/neg} , F4/80 ⁺ , Siglec-F ⁻

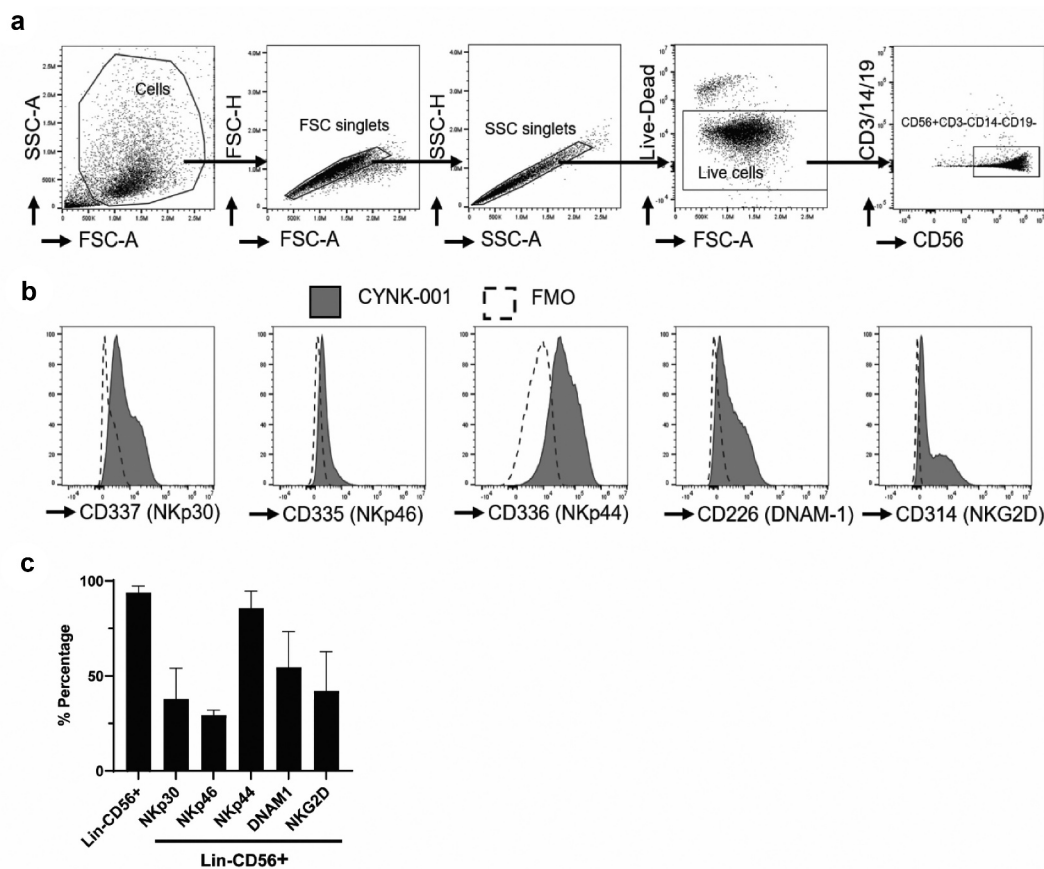


Figure 1. CYNK-001 in vitro characterization. Note: (a) Representative flow cytometry dot plots demonstrating the gating strategy for the analysis of CYNK-001 cells. Thawed CYNK-001 cells were stained with fluorophore-conjugated antibodies recognizing indicated NK cell markers and analyzed by flow cytometry. CYNK-001 are defined as live CD3⁻ CD14⁻ CD19⁻ CD56⁺ cells. (b) Representative histograms of the expression of NK cell activating receptors involved in virus recognition on CYNK-001 cells. FMO—fluorescence minus one control. (c) Quantitative analysis of expression levels of indicated markers on CYNK-001 cells (n=6). Percentage of CD56⁺Lin⁻ under “Live cells” gating as shown in Fig. 1a. Percentage of NKp30, NKp46, NKp44, DNAM-1, and NKG2D is under CD56⁺CD3⁻CD19⁻CD14⁻ gating.

These results suggested a short life span of CYNK-001 cells in immunocompetent Balb/c mice, which might relate to the non-statistically changed viral load (Fig. S3) and the limited effects of CYNK-001 demonstrated in this study.

CYNK-001 reduces lung inflammation induced by IAV infection

Inflammation is one of the essential contributors of IAV-infection disease severity.^{25–27} Therefore, we next examined cytokines and chemokines in the BALF as indications of CYNK-001’s impacts on lung inflammation (Figure 3a). At 3 dpi, no effect of CYNK-001 on murine cytokines and chemokines was observed (Figure 3b). With progression of the disease, the levels of proinflammatory murine cytokines and chemokines showed intensive increase by 6 dpi. For example, IFN- γ level increased from 76 ± 22 pg/ml at 3 dpi to 5633 ± 255 pg/ml at 6 dpi in PBS-treated and IAV-infected mice. Strikingly, CYNK-001-treated mice produced significantly lower level of IFN- γ (1065 ± 367 pg/ml) at 6 dpi, 5-fold less than PBS control group. Consistently, CYNK-001 treatment also reduced other proinflammatory cytokines and chemokines such as MCP-1 ($p < .05$) and IL-6 ($p = .056$). In contrast, levels of TNF- α in BALF remained unchanged upon CYNK-001 treatment.

To further elucidate effects of CYNK-001 in the host immune responses, we profiled immune cell populations in BALF at 3 and 6 dpi. First, unchanged murine CD45⁺ cell populations indicated that CYNK-001 treatment did not alter the total number of immune cell infiltrates in the BALF (Fig. S4). Among murine CD45⁺ cells, host neutrophils and macrophages were most abundant at 3 dpi whereas T cells became the largest immune cell population at 6 dpi in lung (Figure 3c), suggesting the shift from innate to adaptive immune responses. At 3 dpi, CYNK-001-treated mice had $60.6 \pm 2.2\%$ neutrophils, significantly higher than $49.2 \pm 2.9\%$ in PBS-treated mice. By 6 dpi, however, significantly less neutrophils were observed in CYNK-001-treated mice ($12.4 \pm 2.1\%$) compared to PBS control ($19.6 \pm 1.4\%$) (Figure 3d), suggesting a larger reduction of neutrophils in CYNK-001-treated mice along with disease progression. In contrast, CYNK-001 treatment resulted in a significant increase in CD8⁺ T cells at 6 dpi, suggesting its effect on adaptive immune response. As a result, neutrophil-to-CD8⁺ T cell ratio (N8 R), a diagnostic and prognostic marker for severe COVID-19 respiratory disease,^{28–30} was significantly lower in the CYNK-001-treated mice compared to the PBS control (Figure 3e). We also noticed mouse endogenous NK cells were significantly less by CYNK-001 treatment at 3 and 6 dpi (Figure 3d). No significant differences were detected in the

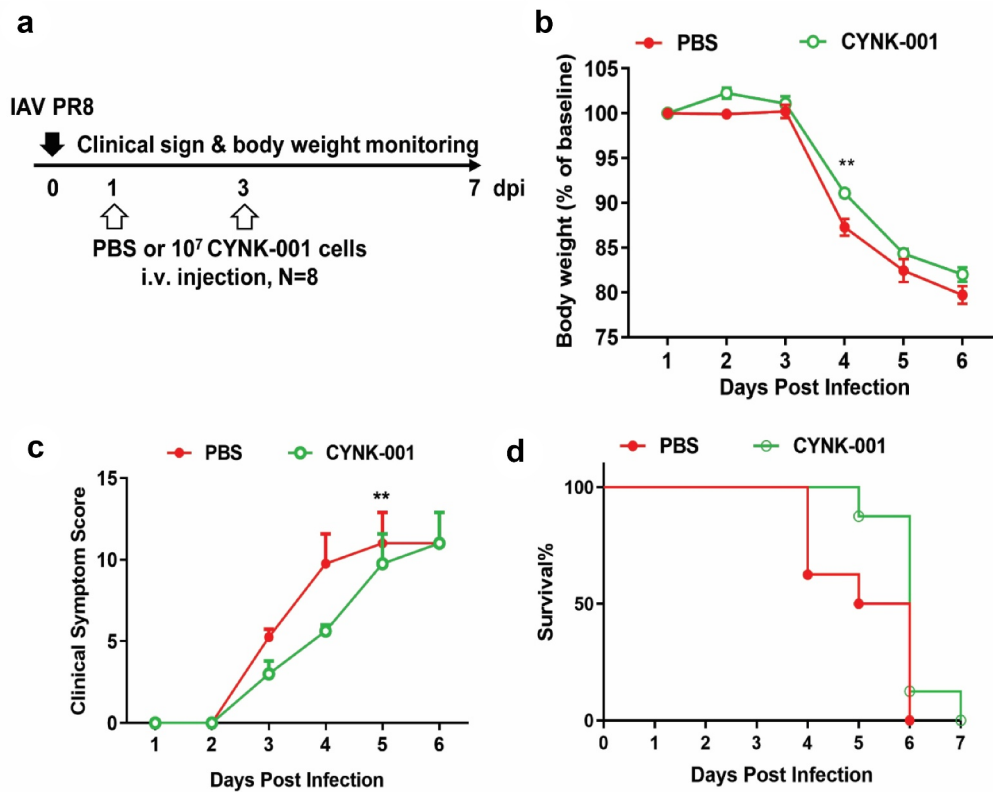


Figure 2. Effects of CYNK-001 in IAV-induced acute and severe infection mouse model. Note: (a) A schematic of the treatment schedule: Balb/c mice were infected with 2500 plaque forming unit (PFU) of influenza A virus (IAV) strain A/Puerto Rico/8/34 (PR8). On day 1 and day 3 post-infection mice were administered 1x10⁷ CYNK-001 cells or PBS intravenously. (b) Body weight change after infection. (c) Clinical score and (d) survival rate of the infected animals with PBS or CYNK-001 treatment (n=8).

number of CD4⁺ T cells and total macrophages, alveolar as well as interstitial macrophages (Fig. S5) at 3 and 6 dpi. Collectively, these data demonstrate the CYNK-001-altered immune responses to viral infection in immunocompetent mice, which overall alleviated inflammation induced by IAV challenge.

CYNK-001 alters murine lung immune cell populations

Compared to uninfected lung tissue, histopathological analysis of the IAV infected lung revealed that the changes in the lungs consisted of necrosis and ulceration of the bronchial lining epithelium, presence of inflammatory exudate in the bronchial lumen, and post-necrotic regenerated epithelium in the bronchi (Fig. S6). No significant difference in microscopic lesions was observed between the groups treated with CYNK-001 and PBS (Table S1). Nevertheless, immunohistochemical analysis of the lungs confirmed a significant increased infiltration of CD3⁺/CD8⁺ T cells co-stained by the two markers in CYNK-001-treated lungs compared to PBS treatment, corroborating with the findings in the BALF, while the amount of CD4⁺/CD8⁺ T cells were comparable between both groups (Figure 4a and 4b). Interestingly, murine CD68⁺ lung macrophages were also significantly increased upon CYNK-001 infusion. These observations suggest the alteration of murine immune cell profiles in lung tissue due to CYNK-001 treatment may contribute to its anti-inflammatory effects post IAV infection.

Discussion

NK cells are critical for innate regulation of the acute phase of IAV infection through cytolytic activity and production of cytokines to directly eliminate virus infected cells^{6,11,31} and for regulation of adaptive immunity.³² In humans, most studies investigating NK cell responses to IAV infection analyzed peripheral blood and lung NK cells from IAV patients or healthy donors in *in vitro* infection models.^{33–35} Here, we report for the first time to our knowledge that adoptive transfer of human NK cells derived from placental hematopoietic stem cells provides protection against severe IAV infection in mice. This effect is presumably via CYNK-001-mediated alleviation of lung inflammation and immunomodulation. It has been reported that NK cell cytolytic activity against influenza virus is triggered by the recognition of viral HA and stress ligands by NKp44 and NKp46 receptors.^{6,31,36} In the current study, antiviral activity of CYNK-001 against IAV infection was not addressed. However, high expression levels of activating receptors in CYNK-001 cells such as NKp44, which is unique compared to peripheral blood NK cells with low or undetectable expression of NKp44,^{24,37–39} suggest our cell product may exhibit cytotoxic response against virus-infected cells through binding activating receptors to viral HA. This hypothesis will be evaluated in further investigations.

NK cell response to IAV has been largely studied in mice, in which protective or detrimental effects were reported due to differences in influenza strain, dose, and genetic background of mice.^{11–13,15–17} The mechanisms underlying different roles that

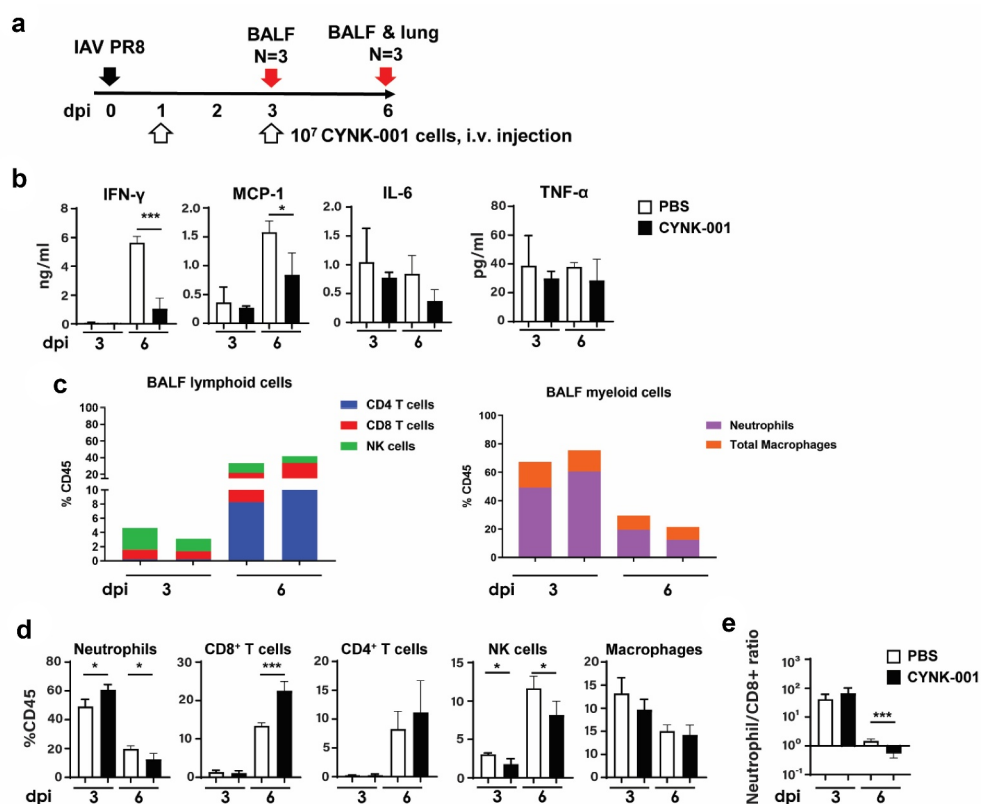


Figure 3. CYNK-001 alters pro-inflammatory cytokine levels and immune cell profile in BALF post IAV-infection. Note: (a) Study schematic: CYNK-001 cells or PBS were treated in Balb/c mice at indicated time points before BALF and lung tissue collection. Pro-inflammatory cytokines (b) and leukocyte subsets (c-e) were analyzed in the bronchial alveolar lavage fluid (BALF) samples of mice at 3 and 6 dpi, using Milliplex and flow cytometry analysis respectively. (c, d) The proportion of indicated murine immune cell subsets as a fraction of CD45+ cells in the BALF. (d) Neutrophil to CD8+ T cell ratio in BALF.

NK cells play in response to IAV infection remain to be elucidated. It is speculated that secretion of cytokines and chemokines from activated NK cells may be a double-edged sword that could promote an antiviral microenvironment but could also induce an intense inflammatory response. The primary mechanisms of IAV pathophysiology include virus replication-induced damage to the respiratory epithelium, the immune responses recruited to handle the spreading virus and subsequent inflammation-induced injuries.⁴⁰ Therefore, one of the keys to combat influenza virus infection is to suppress inflammation without induction of an excessive immune response.

To better understand the effect of CYNK-001 on IAV-induced lung inflammation, an acute severe IAV infection model in Balb/c mice was used in this study. Repeat dosing regimen of CYNK-001 at 1 and 3 dpi was applied to overcome short persistence of CYNK-001 in immunocompetent mice. As observed, vehicle-treated mice started to die as early as 4 dpi, leading to a limited time window for treatment. Therefore, two injections of CYNK-001 within 3 days post infection appeared to be optimal for both dosing frequency and duration in this model. CYNK-001 treatment reduced body weight loss and clinical symptoms and delayed the onset of mortality, thus demonstrating its protective functions *in vivo*. Since the highly dynamic changes of lung viral load and immune cell influxes were presented recently in a murine IAV infection model,⁴¹ the lung viral load examinations in a time-course manner will be helpful to better understand CYNK-001's *in vivo* antiviral activity.

Immune cell infiltration is crucial for control of virus replication and resolution of infection. However, this response often contributes to pathogenesis and morbidity.⁴⁰ In the case of highly pathogenic IAVs such as the 1918 pandemic H1N1 strain and the recent avian H5N1 and H7N9 strains, an excessive inflammatory response caused irreparable damage to the lungs resulting in high mortality rates.^{25–27} To better understand the mechanism underlying CYNK-001-mediated protection against IAV infection, we further investigated the production of cytokines and chemokines as well as immune cell infiltration in the BALF and the lungs. Mice treated with CYNK-001 had decreased pro-inflammatory cytokines and chemokines compared to PBS-treated mice, of which reduction of IFN γ was the most dramatic and significant. In fact, IFN γ -/- mice infected with the H1N1 pandemic virus A/California/04/2009 had decreased immunopathology and enhanced survival,⁴² while a lack of IFN γ signaling in IFN γ R-/- mice infected with the H1N1 virus A/WSN/33 also resulted in decreased virus replication and reduced disease symptoms.⁴³ In addition, IFN γ signaling induces the production of other pro-inflammatory cytokines and chemokines, including TNF α and MCP-1 in macrophages,^{43,44} further suggesting IFN γ as a major driver of inflammatory responses.^{43,45–47} It is reported that MCP-1 recruits monocytes to the lung tissue further worsening the immunopathology.⁴⁸ In line with IFN γ reduction, MCP-1 level was also significantly decreased in CYNK-001-treated mice. Taken together, the significantly

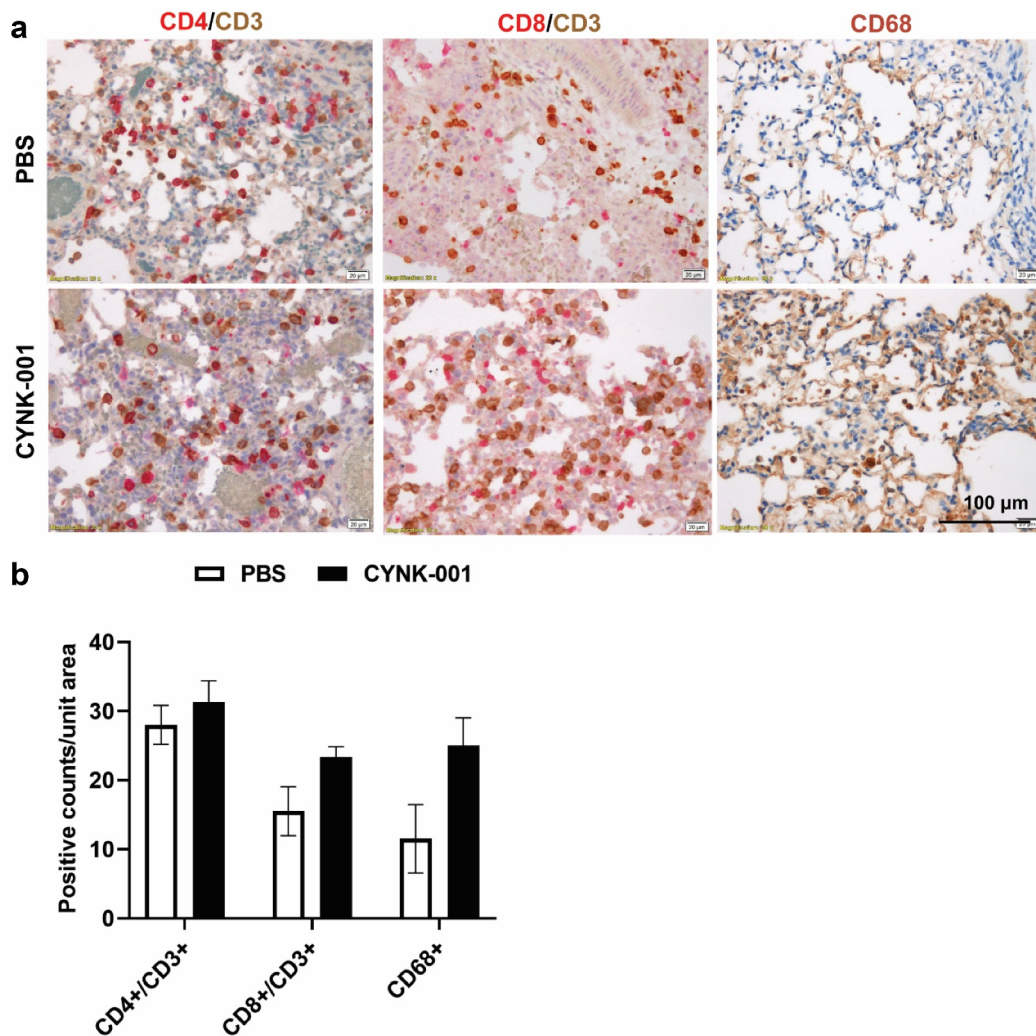


Figure 4. CYNK-001 alters immune cell profiling in lung post IAV-infection. Note: (a) Representative images of lung tissue sections with single staining of mouse CD68 or dual staining of CD3 (DAB, brown) with CD8 or CD4 (AP, red) at dpi 6. (b) Quantitative analysis of cells in per unit area with positively co-stained markers of CD4+/CD3+, CD8+/CD3+, or CD68+ single-stained marker.

reduced proinflammatory cytokines and chemokines such as IFN γ and MCP-1 likely contributed to CYNK-001-mediated anti-inflammatory protection.

High neutrophil-to-lymphocyte ratio (NLR) as well as N8 R have been reported as useful prognostic biomarkers correlated with severe disease and fatality in patients infected with IAV^{49,50} and the SARS-CoV-2 coronavirus.^{28,29} Here, we found that CYNK-001-treated mice had significantly lower N8 R at 6 dpi with reduced neutrophil and increased CD8+ T cells compared to PBS control in BALF, and an increased infiltration of CD3+/CD8+ T cells was also observed in lung tissue post CYNK-001 infusion. These findings suggest a dynamic impact of CYNK-001 treatment on both innate and adaptive immune responses.

With the focus on acute lung injury and inflammation induced by IAV infection, the Balb/c mouse model used in our study was limited in its short in-life duration due to severe symptoms post infection, which prevents the monitoring of chronic impacts of CYNK-001 treatment. In a recent chronic mouse model of mouse-adapted IAV infection, the disease progression and follow-

up symptoms like IAV-associated neuroinflammation, were examined by up to 120 dpi.⁵¹ In addition, the short persistence of CYNK-001 cells when infused in a xenogeneic setting into fully immune competent Balb/c mice was another limitation. Human CD34+ hematopoietic stem cell-engrafted NSG mouse model with transgenic human cytokine expression⁵² may address this issue, and thus better serve the purpose of analyzing long-term therapeutic effects of CYNK-001 cells in future.

In conclusion, we demonstrate that adoptive transfer of CYNK-001 reduces acute lung injury by suppression of inflammation and immunomodulation in a severe IAV-infection model. Our results suggest that CYNK-001 may offer a novel approach to the treatment of viral infections and provide a cohesive scientific rationale for the ongoing Phase I clinical study in COVID-19 patients.

Disclosure statement

J.G., Y.Z., I.R., L.K., S.H., and R.H. were employees of Celularity Inc. when this study was conducted.

Funding

The author(s) reported there is no funding associated with the work featured in this article.

References

- Ferkol T, Schraufnagel D. The global burden of respiratory disease. *Ann Am Thorac Soc*. 2014;11(3):404–06. doi:10.1513/AnnalsATS.201311-405PS.
- Peteranderl C, Herold S, Schmoldt C. Human influenza virus infections. *Semin Respir Crit Care Med*. 2016;37(04):487–500. doi:10.1055/s-0036-1584801.
- Doyle JD, Chung JR, Kim SS, Gaglani M, Raiyani C, Zimmerman RK, Nowalk MP, Jackson ML, Jackson LA, Monto AS, et al. Interim estimates of 2018–19 seasonal influenza vaccine effectiveness — United States, February 2019. *MMWR Morb Mortal Wkly Rep*. 2019;68(6):135–39. doi:10.15585/mmwr.mm6806a2.
- Lanier LL. Evolutionary struggles between NK cells and viruses. *Nat Rev Immunol*. 2008;8(4):259–68. doi:10.1038/nri2276.
- Marofi F, Al-Awad AS, Sulaiman Rahman H, Markov A, Abdelbasset WK, Ivanovna Enina Y, Mahmoodi M, Hassanzadeh A, Yazdanifar M, Stanley Chartrand M, et al. CAR-NK cell: a new paradigm in tumor immunotherapy. *Front Oncol*. 2021;11:673276. doi:10.3389/fonc.2021.673276.
- Arnon TI, Lev M, Katz G, Chernobrov Y, Porgador A, Mandelboim O. Recognition of viral hemagglutinins by NKp44 but not by NKp30. *Eur J Immunol*. 2001;31(9):2680–89. doi:10.1002/1521-4141(200109)31:9<2680::AID-IMMU2680>3.0.CO;2-A.
- Luczo JM, Ronzulli SL, Tompkins SM. Influenza a virus hemagglutinin and other pathogen glycoprotein interactions with NK cell natural cytotoxicity receptors NKp46, NKp44, and NKp30. *Viruses*. 2021;13(2):156. doi:10.3390/v13020156.
- Vivier E, Tomasello E, Baratin M, Walzer T, Ugolini S. Functions of natural killer cells. *Nat Immunol*. 2008;9(5):503–10. doi:10.1038/ni1582.
- Ivanova D, Krempels R, Ryfe J, Weitzman K, Stephenson D, Gingley JP. NK cells in mucosal defense against infection. *Biomed Res Int*. 2014;2014:413982. doi:10.1155/2014/413982.
- Littwitz E, Francois S, Dittmer U, Gibbert K. Distinct roles of NK cells in viral immunity during different phases of acute Friend retrovirus infection. *Retrovirology*. 2013;10:127. doi:10.1186/1742-4690-10-127.
- Gazit R, Gruda R, Elboim M, Arnon TI, Katz G, Achdout H, Hanna J, Qimron U, Landau G, Greenbaum E, et al. Lethal influenza infection in the absence of the natural killer cell receptor gene *Ncr1*. *Nat Immunol*. 2006;7(5):517–23. doi:10.1038/ni1322.
- Nogusa S, Ritz BW, Kassim SH, Jennings SR, Gardner EM. Characterization of age-related changes in natural killer cells during primary influenza infection in mice. *Mech Ageing Dev*. 2008;129(4):223–30. doi:10.1016/j.mad.2008.01.003.
- Stein-Streilein J, Guffee J. In vivo treatment of mice and hamsters with antibodies to asialo GM1 increases morbidity and mortality to pulmonary influenza infection. *J Immunol*. 1986;136:1435–41. [accessed 2021 July 15].
- Kumar P, Thakar MS, Ouyang W, Malarkannan S. IL-22 from conventional NK cells is epithelial regenerative and inflammation protective during influenza infection. *Mucosal Immunol*. 2013;6(1):69–82. doi:10.1038/mi.2012.49.
- Zhou K, Wang J, Li A, Zhao W, Wang D, Zhang W, Yan J, Gao GF, Liu W, Fang M, et al. Swift and strong NK cell responses protect 129 mice against high-dose influenza virus infection. *J Immunol*. 2016;196(4):1842–54. doi:10.4049/jimmunol.1501486.
- Abdul-Careem MF, Mian MF, Yue G, Gillgrass A, Chenoweth MJ, Barra NG, Chew MV, Chan T, Al-Garawi AA, Jordana M, et al. Critical role of natural killer cells in lung immunopathology during influenza infection in mice. *J Infect Dis*. 2012;206(2):167–77. doi:10.1093/infdis/jis340.
- Zhou G, Juang SW, Kane KP. NK cells exacerbate the pathology of influenza virus infection in mice. *Eur J Immunol*. 2013;43(4):929–38. doi:10.1002/eji.201242620.
- Jost S, Quillay H, Reardon J, Peterson E, Simmons RP, Parry BA, Bryant NNP, Binder WD, Altfeld M, et al. Changes in cytokine levels and NK cell activation associated with influenza. *PLoS One*. 2011;6(9):e25060. doi:10.1371/journal.pone.0025060.
- Denney L, Aitken C, Li CK, Wilson-Davies E, Kok WL, Clelland C, Rooney K, Young D, Dong T, McMichael AJ, et al. Reduction of natural killer but not effector CD8 T lymphocytes in three consecutive cases of severe/lethal H1N1/09 influenza a virus infection. *PLoS One*. 2010;5(5):e10675. doi:10.1371/journal.pone.0010675.
- Fox A, Le NM, Horby P, van Doorn HR, Nguyen VT, Nguyen HH, Cap NT, Phu VD, Ha NM, Ngoc DNT, et al. Severe pandemic H1N1 2009 infection is associated with transient NK and T deficiency and aberrant CD8 responses. *PLoS One*. 2012;7(2):e31535. doi:10.1371/journal.pone.0031535.
- Spanholtz J, Tordoier M, Eissens D, Preijers F, van der Meer A, Joosten I, Schaap N, de Witte TM, Dolstra H, et al. High log-scale expansion of functional human natural killer cells from umbilical cord blood CD34-positive cells for adoptive cancer immunotherapy. *PLoS One*. 2010;5(2):e9221. doi:10.1371/journal.pone.0009221.
- Szretter KJ, Balish AL, Katz JM. Influenza: propagation, quantification, and storage. *Curr Protoc Microbiol*. 2006;3(1). Chapter 15: Unit 15G 1. doi:10.1002/0471729256.mc15g01s3.
- Yu YR, O’Koren EG, Hotten DF, Kan MJ, Kopin D, Nelson ER, Que L, Gunn MD. A protocol for the comprehensive flow cytometric analysis of immune cells in normal and inflamed murine non-lymphoid tissues. *PLoS One*. 2016;11(3):e0150606. doi:10.1371/journal.pone.0150606.
- Kang L, Voskianarian-Berse V, Law E, Reddin T, Bhatia M, Hariri A, Ning Y, Dong D, Maguire T, Yarmush M, et al. Characterization and ex vivo expansion of human placenta-derived natural killer cells for cancer immunotherapy. *Front Immunol*. 2013;4:101. doi:10.3389/fimmu.2013.00101.
- Gao R, Bhatnagar J, Blau DM, Greer P, Rollin DC, Denison AM, DeLeon-Carnes M, Shieh W-J, Sambhara S, Tumpey TM, et al. Cytokine and chemokine profiles in lung tissues from fatal cases of 2009 pandemic influenza A (H1N1): role of the host immune response in pathogenesis. *Am J Pathol*. 2013;183(4):1258–68. doi:10.1016/j.ajpath.2013.06.023.
- Koutsakos M, Kedzierska K, Subbarao K. Immune responses to Avian influenza viruses. *J Immunol*. 2019;202(2):382–91. doi:10.4049/jimmunol.1801070.
- Wang Z, Loh L, Kedzierski L, Kedzierska K. Avian influenza viruses, inflammation, and CD8(+) T cell immunity. *Front Immunol*. 2016;7:60. doi:10.3389/fimmu.2016.00060.
- Liu Y, Du X, Chen J, Jin Y, Peng L, Wang HHX, Luo M, Chen L, Zhao Y. Neutrophil-To-Lymphocyte ratio as an independent risk factor for mortality in hospitalized patients with COVID-19. *J Infect*. 2020;81(1):e6–e12. doi:10.1016/j.jinf.2020.04.002.
- Lagunas-Rangel FA. Neutrophil-To-Lymphocyte ratio and lymphocyte-to-C-reactive protein ratio in patients with severe coronavirus disease 2019 (COVID-19): a meta-analysis. *J Med Virol*. 2020;92(10):1733–34. doi:10.1002/jmv.25819.
- Carissimo G, Xu W, Kwok I, Abdad MY, Chan YH, Fong SW, Puan KJ, Lee CYP, Yeo NKW, Amrun SN, et al. Whole blood immunophenotyping uncovers immature neutrophil-to-VD2 T-cell ratio as an early marker for severe COVID-19. *Nat Commun*. 2020;11(1):5243. doi:10.1038/s41467-020-19080-6.
- Mandelboim O, Lieberman N, Lev M, Paul L, Arnon TI, Bushkin Y, Davis DM, Strominger JL, Yewdell JW, Porgador A, et al. Recognition of haemagglutinins on virus-infected cells by NKp46 activates lysis by human NK cells. *Nature*. 2001;409(6823):1055–60. doi:10.1038/35059110.
- Waggoner SN, Cornberg M, Selin LK, Welsh RM. Natural killer cells act as rheostats modulating antiviral T cells. *Nature*. 2011;481(7381):394–98. doi:10.1038/nature10624.

33. Kronstad LM, Seiler C, Vergara R, Holmes SP, Blish CA. Differential induction of IFN- α and modulation of CD112 and CD54 expression govern the magnitude of NK cell IFN- γ response to Influenza A viruses. *J Immunol.* 2018;201(7):2117–31. doi:10.4049/jimmunol.1800161.
34. Juarez-Reyes A, Noyola DE, Monsivais-Urenda A, Alvarez-Quiroga C, Gonzalez-Amaro R. Influenza virus infection but not H1N1 influenza virus immunization is associated with changes in peripheral blood NK cell subset levels. *Clin Vaccine Immunol.* 2013;20(8):1291–97. doi:10.1128/CVI.00194-13.
35. Cooper GE, Ostridge K, Khakoo SI, Wilkinson TMA, Staples KJ. Human CD49a(+) lung natural killer cell cytotoxicity in response to Influenza A virus. *Front Immunol.* 2018;9:1671. doi:10.3389/fimmu.2018.01671.
36. Arnon TI, Achdout H, Lieberman N, Gazit R, Gonen-Gross T, Katz G, Bar-Ilan A, Bloushtain N, Lev M, Joseph A, et al. The mechanisms controlling the recognition of tumor- and virus-infected cells by NKp46. *Blood.* 2004;103(2):664–72. doi:10.1182/blood-2003-05-1716.
37. Ferlazzo G, Thomas D, Lin SL, Goodman K, Morandi B, Muller WA, Moretta A, Münz C. The abundant NK cells in human secondary lymphoid tissues require activation to express killer cell Ig-like receptors and become cytolytic. *J Immunol.* 2004;172(3):1455–62. doi:10.4049/jimmunol.172.3.1455.
38. Vitale M, Bottino C, Sivori S, Sanseverino L, Castriconi R, Marcenaro E, Augugliaro R, Moretta L, Moretta A. Nkp44, a novel triggering surface molecule specifically expressed by activated natural killer cells, is involved in non-major histocompatibility complex-restricted tumor cell lysis. *J Exp Med.* 1998;187(12):2065–72. doi:10.1084/jem.187.12.2065.
39. Guo X, Mahlakoiv T, Ye Q, Somanchi S, He S, Rana H, DiFiglia A, Gleason J, van der Touw W, Hariri R, et al. CBLB ablation with CRISPR/Cas9 enhances cytotoxicity of human placental stem cell-derived NK cells for cancer immunotherapy. *J Immunother Cancer.* 2021;9(3):e001975. doi:10.1136/jitc-2020-001975.
40. Alon R, Sportiello M, Kozlovski S, Kumar A, Reilly EC, Zarbock A, Garbi N, Topham DJ. Leukocyte trafficking to the lungs and beyond: lessons from influenza for COVID-19. *Nat Rev Immunol.* 2021;21(1):49–64. doi:10.1038/s41577-020-00470-2.
41. Myers MA, Smith AP, Lane LC, Moquin DJ, Aogo R, Woolard S, Thomas P, Vogel P, Smith AM. Dynamically linking influenza virus infection kinetics, lung injury, inflammation, and disease severity. *Elife.* 2021;10:10. doi:10.7554/eLife.68864.
42. Califano D, Furuya Y, Roberts S, Avram D, McKenzie ANJ, Metzger DW. IFN- γ increases susceptibility to influenza a infection through suppression of group II innate lymphoid cells. *Mucosal Immunol.* 2018;11(1):209–19. doi:10.1038/mi.2017.41.
43. Nicol MQ, Campbell GM, Shaw DJ, Dransfield I, Ligertwood Y, Beard PM, Nash AA, Dutia BM. Lack of IFN γ signaling attenuates spread of influenza a virus in vivo and leads to reduced pathogenesis. *Virology.* 2019;526:155–64. doi:10.1016/j.virol.2018.10.017.
44. Hui KP, Lee SM, Cheung CY, Ng IH, Poon LL, Guan Y, Ip NYY, Lau ASY, Peiris JSM. Induction of proinflammatory cytokines in primary human macrophages by influenza a virus (H5N1) is selectively regulated by IFN regulatory factor 3 and p38 MAPK. *J Immunol.* 2009;182(2):1088–98. doi:10.4049/jimmunol.182.2.1088.
45. Liu B, Bao L, Wang L, Li F, Wen M, Li H, Deng W, Zhang X, Cao B. Anti-IFN- γ therapy alleviates acute lung injury induced by severe influenza a (H1N1) pdm09 infection in mice. *J Microbiol Immunol Infect.* 2021;54(3):396–403. doi:10.1016/j.jmii.2019.07.009.
46. Weiss ID, Wald O, Wald H, Beider K, Abraham M, Galun E, Nagler A, Peled A. IFN- γ treatment at early stages of influenza virus infection protects mice from death in a NK cell-dependent manner. *J Interferon Cytokine Res.* 2010;30(6):439–49. doi:10.1089/jir.2009.0084.
47. Karupiah G, Chen JH, Mahalingam S, Nathan CF, MacMicking JD. Rapid interferon γ -dependent clearance of Influenza A virus and protection from consolidating pneumonitis in nitric oxide Synthase 2-deficient mice. *J Exp Med.* 1998;188(8):1541–46. doi:10.1084/jem.188.8.1541.
48. Deshmane SL, Kremlev S, Amini S, Sawaya BE. Monocyte chemoattractant protein-1 (MCP-1): an overview. *J Interferon Cytokine Res.* 2009;29(6):313–26. doi:10.1089/jir.2008.0027.
49. Indavarapu A, Akinapelli A. Neutrophils to lymphocyte ratio as a screening tool for swine influenza. *Indian J Med Res.* 2011;134:389–91. [accessed 2021 Jul 15].
50. Zhang Y, Zou P, Gao H, Yang M, Yi P, Gan J, Shen Y, Wang W, Zhang W, Li J, et al. Neutrophil-lymphocyte ratio as an early new marker in AIV-H7N9-infected patients: a retrospective study. *Ther Clin Risk Manag.* 2019;15:911–19. doi:10.2147/TCRM.S206930.
51. Hosseini S, Wilk E, Michaelsen-Preusse K, Gerhauser I, Baumgartner W, Geffers R, Schughart K, Korte M. Long-Term neuroinflammation induced by Influenza A virus infection and the impact on Hippocampal neuron morphology and function. *J Neurosci.* 2018;38(12):3060–80. doi:10.1523/JNEUROSCI.1740-17.2018.
52. Wunderlich M, Chou FS, Sexton C, Presicce P, Chougnat CA, Aliberti J, Mulloy JC. Improved multilineage human hematopoietic reconstitution and function in NSGS mice. *PLoS One.* 2018;13(12):e0209034. doi:10.1371/journal.pone.0209034.